Holocene left-slip rate determined by cosmogenic surface dating on the Xidatan segment of the Kunlun fault (Qinghai, China)

J. Van der Woerd — Laboratoire de Tectonique, Mécanique de la Lithosphère, URA 1093, Institut de Physique du Globe de Paris, 4 Place Jussieu, 75252 Paris Cedex 05, France, *and* Institute of Geophysics and Planetary Physics, Lawrence Livermore National Laboratory, Livermore, California 94550
F. J. Ryerson — Institute of Geophysics and Planetary Physics, Lawrence Livermore National Laboratory, Livermore, California 94550
P. Tapponnier, Y. Gaudemer — Laboratoire de Tectonique, Mécanique de la Lithosphère, URA 1093, Institut de Physique du Globe de Paris, 4 Place Jussieu, 75252 Paris Cedex 05, France
R. Finkel — Institute of Geophysics and Planetary Physics, Lawrence Livermore National Laboratory, Livermore, California 94550
A. S. Meriaux — Laboratoire de Tectonique, Mécanique de la Lithosphère, URA 1093, Institut de Physique du Globe de Paris, 4 Place Jussieu, 75252 Paris Cedex 05, France, *and* Institute of Geophysics and Planetary Physics, Lawrence Livermore National Laboratory, Livermore, California 94550
M. Caffee — Institute of Geophysics and Planetary Physics, Lawrence Livermore National Laboratory, Livermore, California 94550
Zhao Guoguang, He Qunlu — Institute of Crustal Dynamics, State Seismological Bureau, Beijing 100085, People's Republic of China

ABSTRACT

Cosmogenic dating, using in situ ^{26}Al and ^{10}Be in quartz pebbles from alluvial terrace surfaces, constrains the late Holocene slip rate on the Xidatan segment of the Kunlun fault in northeastern Tibet. Two terrace risers offset by 24 ± 3 and 33 ± 4 m, having respective ages of 1788 ± 388 and 2914 ± 471 yr, imply a slip rate of 12.1 ± 2.6 mm/yr. The full range of ages obtained (≤22.8 k.y., most of them between 6.7 and 1.4 k.y.) confirm that terrace deposition and incision, hence landform evolution, are modulated by post-glacial climate change. Coupled with minimum offsets of 9–12 m, this slip rate implies that great earthquakes (M ~8) with a recurrence time of 800–1000 yr, rupture the Kunlun fault near 94°E.

INTRODUCTION

Competing models of large-scale deformation during continental collision (see Peltzer and Saucier, 1996, for a review) differ in several key aspects. One is the relative amount of shortening absorbed by thrusts and by strike-slip faults. Another is the proportion of strain taken up by large faults as opposed to that distributed within the blocks they separate. Any quantitative assessment of strain localization or partitioning requires accurate knowledge of slip rates along active thrusts and strike-slip faults. In this paper we present results of cosmogenic nuclide dating of offset alluvial terraces, at one site near the eastern end of Xidatan Valley (Fig. 1) that enable us to constrain the late Holocene slip rate on the Kunlun fault in northeastern Tibet, one of the largest left-lateral strike-slip faults of the India-Asia collision zone (Tapponnier and Molnar, 1977).

GEOLOGIC AND GEOMORPHIC FRAMEWORK

The Xidatan pull-apart trough is floored by a broad Quaternary bajada fed by north-flowing drainage catchments with headwaters in the Burhan Budai Mountain range. This ice-capped range peaks above 6000 m, and is chiefly built of folded turbidites and phyllites belonging to the Triassic Songpan Garze terrane of eastern Tibet (Chang et al., 1986). Present-day glaciers flowing down the north slope of the range stop short of the Xidatan trough. There is no clear evidence of glacial deposits in Xidatan, which implies that the ice tongues in the latest Pleistocene did not cross the active Kunlun fault trace.

The fault trace cuts across the fans of the north-sloping bajada, and is marked by large, stepping sag-ponds and pressure ridges. Commonly, risers of inset alluvial terraces are offset laterally 10 to 100 m by the fault (Kidd and Molnar, 1988). Despite the seismically disrupted morphology, there is no historical or instrumental record of recent earthquakes in the area (Gongxu et al., 1989).

SITE DESCRIPTION: INSET TERRACES AND RISER OFFSETS

The site studied here is located near the eastern end of Xidatan, at the outlet of a stream fed by glacial meltwaters (Figs. 1 and 2). The corresponding glacier tongue extends from ~5500 m to ~4800 m. The apex of the stream fan is at an elevation of 4300 m, roughly that of the permafrost line (Derbyshire, 1987).

The stream is now entrenched within inset terraces along the west side of its largest, oldest fan, which is thinly sprinkled with loess—light gray on SPOT ("Satellite for Observation of the Earth" [French]) image, Fig. 3A—as typical of most streams in Xidatan. Large alluvial fans first formed at the outlet of the lowermost moraines, and were then incised by, and hence protected from further action of the stream. Continued incision led to the abandonment of several terraces and new fans forming downstream from the older ones. We infer that such stepwise, northward progradation of deposition is due to stream profile adjustment, in tune with the wet, warm climatic episode that followed deglaciation; i.e., the early Holocene optimum, now identified in various parts of Asia (Gasse et al., 1991; Pachur et al., 1995), and the subsequent, drier period.

There are three main terrace levels at the site: T0 is the active flood plain, T1′ is the terrace last abandoned by the stream, T1 is a first strath terrace ~1.70 m above the stream bed, and T2 is a second strath terrace, ~2.5 m above T1 (Fig. 3B). T3 is the highest level, corresponding to the ancient fan surface, about 5.5 m above T2, and is incised by small gullies or rills. Although T1 is now clearly abandoned by the stream, its western riser south of the fault trace is not well defined, and its surface occupied by a wet, marshy area (dark region on SPOT image, Fig. 3A). All of the terrace surfaces are paved with relatively small, well-rounded and sorted pebbles and cobbles (Fig. 2). Both of the principal risers (T2/T1 and T3/T2) are offset by the fault (Fig. 3). Our measurements of the riser offsets (with a tape in the field, corroborated by air photo and SPOT image interpretation), are 24 ± 3 m and 33 ± 4 m, respectively. A sagpond on T2, and a pressure ridge on T3 (Fig. 2) make more accurate measurement difficult. The particularly large sags and pressure ridges on T3 (Fig. 3A) imply cumulative ground deformation by great earthquakes. On T2, such features are smaller and smoother, and there are no clear mole tracks on T1 (Fig. 3, A and B).

SAMPLING AND COSMOGENIC DATING

Samples weighing 30–300 g (most commonly ~100 g), lying on the surface or sometimes partially embedded in it, were collected on T1, T2, and T3 along two traverses parallel to the fault (Fig. 3B). We processed 29 samples for ^{10}Be and ^{26}Al cosmic ray exposure dating (cf. Lal, 1991); 13 on T1, 10 on T2, and 6 on T3. Quartz was separated and purified using the methods described by Kohl and Nishiizumi (1992), and the ratios of cosmogenic ^{26}Al and ^{10}Be to stable isotopes were determined by accelerator mass spectrometry (AMS) at the Lawrence Livermore National Laboratory (LLNL)-AMS facility. The cosmo-

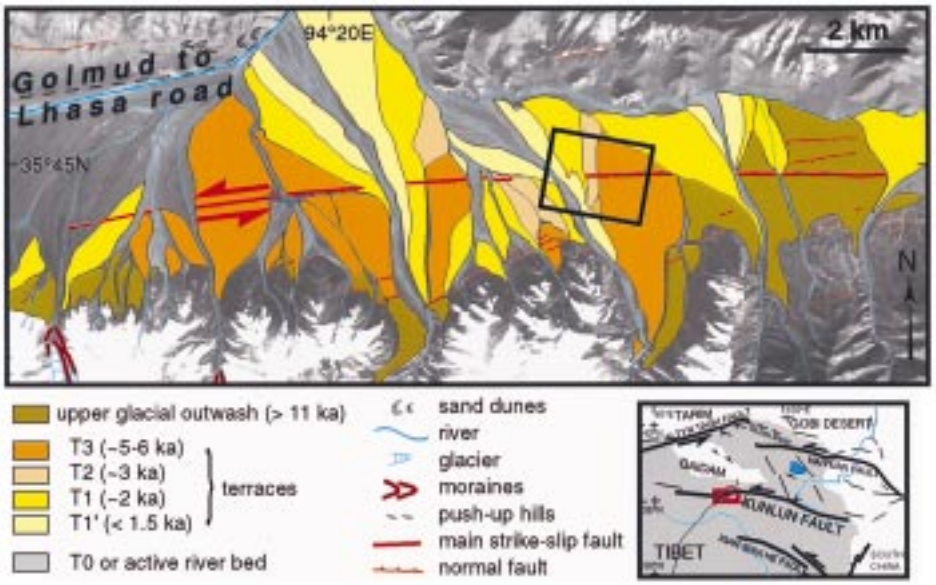

Figure 1. Geomorphic map of alluvial fans and terraces cut by Kunlun Fault in central Xidatan. Bold box indicates location of site in Figures 2 and 3. Box shows location of area in broader framework of northeastern Tibet recent tectonics.

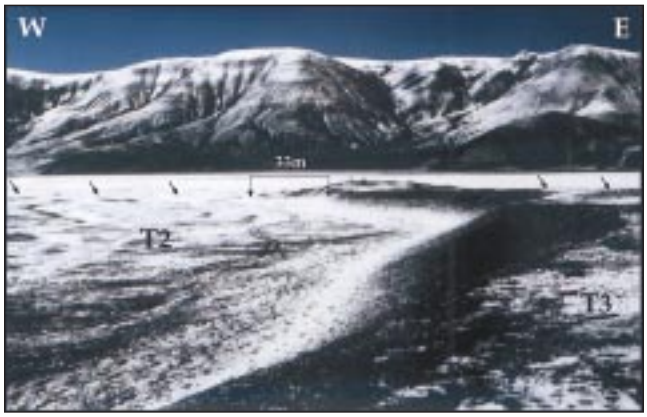

Figure 2. View from top of T3 looking toward north, upstream from study site, of dogleg, left-lateral offset of T3/T2 riser. Person (~1.8 m tall), on top right of pressure ridge in central part of dogleg gives scale. Note alluvial pebbles and cobbles on terrace surface. Black arrows indicate fault trace.

genic production rates used here are those of Nishiizumi (1989), corrected for altitude and latitude (Lal, 1991). Model ages are calculated assuming zero erosion (Table 1).

The large majority of the ^{26}Al and ^{10}Be model ages are concordant (within 10%) with simple exposure histories and negligible erosion. Samples younger than 500 yr (from the youngest population on the lower terrace, T1) show greater discordance, however, due to larger relative errors on the age associated with low cosmogenic nuclide abundance (~2×10^4 atoms $\cdot$ g^{-1}). Given the otherwise good agreement between the ^{26}Al and ^{10}Be ages, we will use the mean Al-Be age in the following discussion (except for sample KL3D(d)), for which low ion currents and small sample size prevented the determination of an ^{26}Al age). The ages obtained for each terrace are similar whether the sample is upstream or downstream of the fault. Hence, for each terrace we group the sample populations from both sides of the fault (Fig. 3C).

T1 is the only terrace displaying a clear bimodal distribution of ages. The youngest samples have ages ranging from ~200 to ~500 yr (mean = 278 ± 87 yr). We interpret these samples to reflect the occurrence of a single, recent depositional event, probably a centennial flash flood that invaded and washed part of T1, redepositing material from the flood plain onto its surface and eroding earthquake mole tracks. We infer the ages of four samples on the eastern half of that terrace (1778 ± 388 yr; Fig. 3C) to reflect the time at which its surface ceased to be the permanent flood plain of the river. That these older ages are retrieved on the eastern side of the terrace indicates that this flash flood did not rework the entire surface of T1, particularly near its outer riser, and hence did not modify the offset of the T1/T2 riser.

Most sample ages on each terrace show no overlap with those on others (Table 1), and tend to cluster about distinct, mean values (1778 ± 388 yr, 2914 ± 471 yr and 5106 ± 290 yr) that increase with elevation. Four samples, however, are much older than all the others. One, on T1, is >4 k.y. older than 1778 yr. Two, on T2, are >4 and >8.5 k.y. older than 2914 yr, and the oldest, on T3, is >17 k.y. older than 5106 yr. These samples probably represent reworked material from older deposits upstream. The westward decrease and dispersion of ages within each terrace sample set may indicate that their surfaces continued to evolve as westward terrace abandonment progressed, with diachronic mixing in the upper several tens of centimeters near the surface.

The younger samples found on terrace T1 (278 ± 87 yr) place an upper limit on inherited cosmogenic nuclide concentration and indicate that both bedrock exhumation and fluvial transport must have been rapid. For instance, in the steady-state erosion approximation, an inherited component equivalent to 500 yr of surface exposure implies a bedrock exhumation on the order of 1 mm/yr. Similarly, rapid fluvial transport is consistent with the relatively steep, small catchment and short distance between the range crest and the sampled terrace surfaces (≤ 10 km, and an average slope gradient of ~4°).

Strath terrace risers are constantly rejuvenated by river flow along their base. Consequently, only when the terrace level at the base of a riser is abandoned can this riser begin to act as a passive marker and record displacement by a fault. We relate the offsets of the T3/T2 and T2/T1 risers to the mean ages of T2 and T1, respectively. The Kunlun fault would therefore have offset the T3/T2 riser by 33 ± 4 m in 2914 ± 471 yr, and the T2/T1 riser by 24 ± 3 m in 1778 ± 388 yr. Both offsets yield fairly consistent slip rates (11.3 ± 3.2 and 13.5 ± 4.6 mm/yr) that constrain the late Holocene left-slip rate along the fault in east Xidatan, calculated as the weighted mean of both slip rates to be 12.1 ± 2.6 mm/yr (Fig. 4).

If 1778 and 2914 yr were the ages of large flash floods that resurfaced T1 and T2 without reshaping the T2/T1 and T3/T2 risers, the youngest pebbles on T3 and T2 might be used to estimate upper age limits for the T3/T2 and T2/T1 risers. Such ages, 4852 ± 702 and 2414 ± 375 yr, would yield minimum slip rates of 9.9 ± 2.8 and 6.8 ± 1.8 mm/yr, respectively. The unimodal distribution of surface ages on T2, however, makes this interpretation unlikely.

DISCUSSION AND IMPLICATIONS: SEISMIC BEHAVIOR OF THE KUNLUN FAULT AND REGIONAL CLIMATE CHANGE

The slip rate derived here is consistent with those inferred in other studies. Zhao (1996) in particular, documented 10 offsets of gullies and terrace risers in Xidatan, ranging from 10 to 152 m, and retrieved seven thermoluminescence or ^{14}C ages, ranging from 2.14 ka to 12.0 ka, with uncertainties of 6%–9%. From this, they derived a Holocene slip rate of about 11.5 mm/yr, but without error estimates on the offsets, the uncertainty on that rate cannot be assessed. The long-term Pleistocene average rate estimated by Kidd and Molnar (1988; 10–20 mm/yr), loosely brackets both our and Zhao's (1996) values. In a strict sense, however, it cannot be simply compared

with either, because it is deduced from the separation of lower-Pleistocene moraines south and east of the Kunlun Pass from a presumed source in the mountains to the west. To the large uncertainty in the age of the lake beds that overlie the moraine (2.8–1.5 Ma), one should add ~30% error on the offset, due to poor definition of the eastern piercing point (Kidd and Molnar, 1988, Fig. 6).

The fast 12.1 mm/yr late Holocene rate we obtain confirms that slip on the Kunlun fault takes up a large fraction of the eastward component of motion of Tibet relative to the Gobi at 94.5°E (e.g., Peltzer and Saucier, 1996). When combined with evidence at adjacent sites, the temporal evolution of the terrace surfaces, and the offsets of their risers, shed light on the seismic behavior of the Kunlun fault across Xidatan. The very large mole tracks on the high terraces and their absence on the low terraces require the occurrence of rare, great earthquakes. At six sites, our tape measurements yielded minimum offsets of 9 to 12 m, compatible with that (10 m) found by Kidd and Molnar (1988) and Zhao (1996). At eight sites, we found cumulative offsets two or three times 9, 11, and 12 m. The cumulative offsets here imply that two M ~8 earthquakes having individual displacements of 11–12 m might have offset the T2/T1 riser in the past ~1800 yr, and three such earthquakes might be responsible for the offset of the T3/T2 riser in the past ~2900 yr. In keeping with this interpretation, one rill channel offset of about 50 m, and the particularly large pressure ridges and sag ponds on top of T3 (Figs. 2 and 3), might be the cumulative result of about five great earthquakes in the past ~5100 yr (Fig. 3B). Results from trenching elsewhere in Xidatan (Zhao, 1996) are compatible with the occurrence of 4 earthquakes in the last 4000 yr. Clearly, the last event took place prior to the flash flood on T1 278 ± 87 yr ago. Overall, the quantitative evidence suggests the occurrence of great, characteristic earthquakes with a recurrence interval of ~800–1000 yr.

The ages obtained improve our understanding of the relationship between terrace deposition and incision and climatic change (e.g. Gaudemer et al., 1995). The oldest pebble found (KL4U[1], 22.8 k.y.) probably originated in the last glacial maximum moraine upstream from the site. The other sample ages, including the outliers (from 11 515 ± 1727 yr onward), are younger than the postglacial warming at 14.5 ka, with most ages between 6719 ± 1022 and 1452 ± 237 yr. This is compatible with evidence from pollen in cores of the Dunde Ice Cap, ~300 km to the northeast, which indicates that the summer monsoon extended into northeast Tibet during the first half of the Holocene (Liu et al., 1998), and that the subsequent climate was more arid with intervening humid periods (e.g. Gasse et al., 1991). Terrace emplacement and incision in Xidatan were thus coeval with a period of fluctuating precipitation. That landform evolution in the area was modulated by climate variability contradicts the

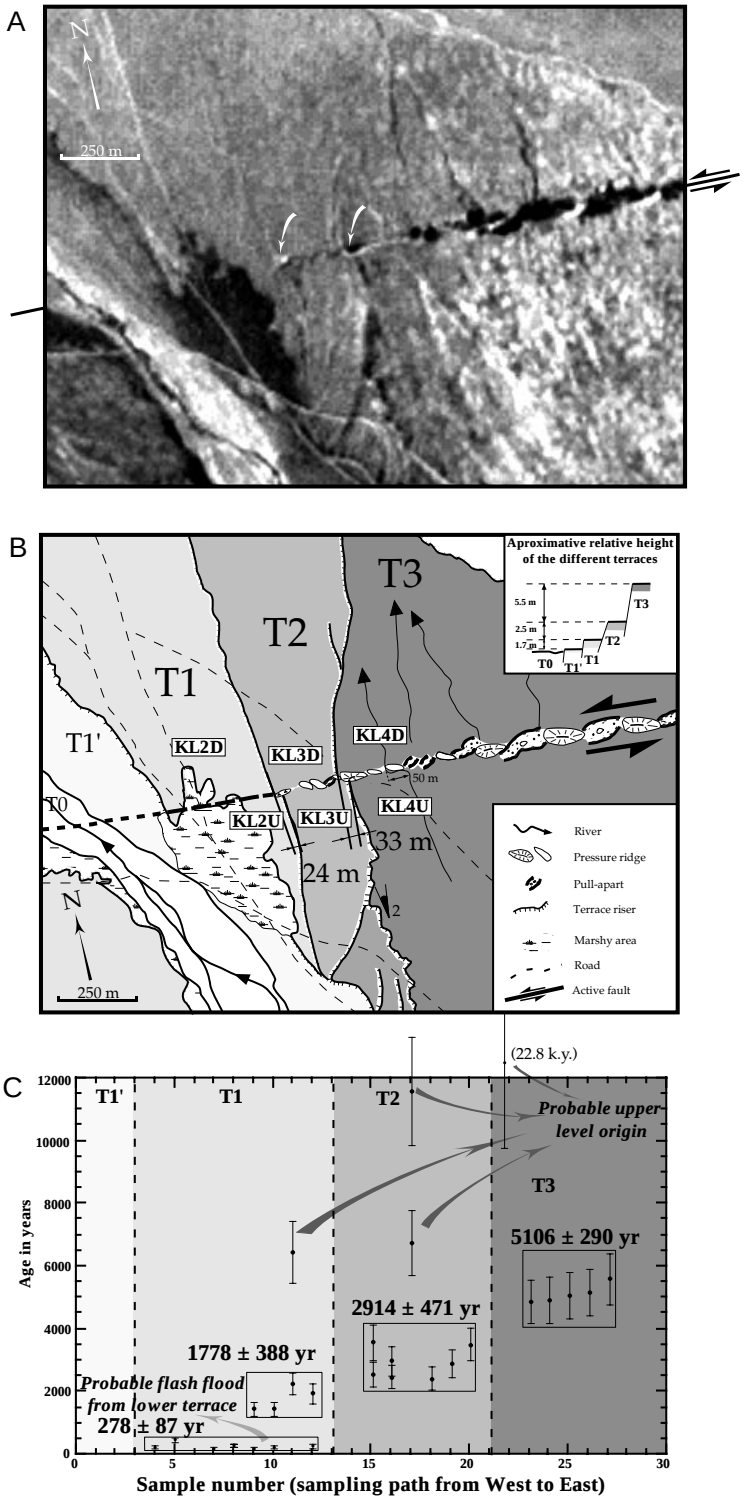

Figure 3. A: Enlargement of panchromatic (10 m pixel) SPOT image (KJ237-278) of site area. Older fan surface (T3) is clear from spotted, light gray to white hue. Stepping earthquake pressure ridges and sag ponds (enhanced by shadows) are much larger on T3 than on T2, and disappear altogether on T1 and T1′. White arrows show offsets of two principal terrace risers. B: Schematic interpretation of image enlargement in A. Alluvial surfaces are numbered as function of increasing height (inset) and age, starting in active stream flood plain (T0) to left. Riser and channel offsets were measured in field, on air photos, and SPOT image. Fist-size quartz pebbles were sampled on top of main alluvial surfaces, south and north of fault trace. C: Plot of sample ages, for each terrace, in relative position, from west to east. For each terrace level, samples were grouped and mean age was calculated (boxes and bold numbers, see discussion in text). Light and dark arrows indicate flash floods and outliers, respectively. Note slight, systematic decrease in ages (~1000 yr) on each terrace from east to west.

TABLE 1. ANALYTICAL RESULTS OF COSMOGENIC DATING OF 29 SAMPLES AT STUDY SITE.

Sample*	^{10}Be§ (10^5 atoms.g^{-1})	^{26}Al§ (10^5 atoms.g^{-1})	^{10}Be model age# (yr)	^{26}Al model age# (yr)	Average$ (yr)	Ratio $^{26}Al/^{10}Be$
Surface T1						
KL2D(a)	0.225 ± 0.06	1.18 ± 0.135	265 ± 88	228 ± 57	239 ± 48	0.86
KL2D(b)	0.473 ± 0.037	2.14 ± 0.157	558 ± 120	414 ± 97	471 ± 76	0.74
KL2D(d)	0.137 ± 0.046	1.29 ± 0.168	162 ± 63	250 ± 65	205 ± 45	1.55
KL2D(e)	0.258 ± 0.027	1.41 ± 0.124	304 ± 69	273 ± 65	288 ± 47	0.90
KL2D(f)	0.149 ± 0.025	1.13 ± 0.23	176 ± 46	218 ± 66	190 ± 38	1.24
KL2D(g)	1.25 ± 0.051	7.52 ± 0.264	1476 ± 301	1455 ± 329	1467 ± 222	0.99
KL2D(h)	1.76 ± 0.076	13.1 ± 0.610	2073 ± 424	2536 ± 553	2245 ± 337	1.22
KL2D(i)	0.493 ± 0.113	1.26 ± 0.125	582 ± 177	244 ± 60	279 ± 57	0.42
KL2U(a)	1.61 ± 0.069	10.5 ± 1.37	1901 ± 389	2035 ± 526	1948 ± 313	1.07
KL2U(b)	5.50 ± 0.093	32.6 ± 1.03	6495 ± 1304	6332 ± 1430	6421 ± 963	0.97
KL2U(c)	0.204 ± 0.033	1.34 ± 0.138	241 ± 62	260 ± 64	250 ± 44	1.08
KL2U(d)	1.25 ± 0.123	7.35 ± 0.617	1478 ± 329	1423 ± 340	1452 ± 237	0.96
KL2U(e)	0.31 ± 0.023	1.33 ± 0.097	366 ± 78	258 ± 61	299 ± 48	0.71
Surface T2						
KL3D(a)	2.17 ± 0.103	13.2 ± 0.614	2556 ± 526	2550 ± 582	2553 ± 390	1.00
KL3D(b)	2.08 ± 0.068	12.9 ± 0.485	2454 ± 497	2508 ± 569	2477 ± 374	1.02
KL3D(c)	9.74 ± 0.194	59.2 ± 1.59	11516 ± 2315	11514 ± 2593	11515 ± 1727	1.00
KL3D(d)	3.16 ± 0.178	N.D.†	3727 ± 774	N.D.	N.D.	N.D.
KL3D(e)	2.48 ± 0.095	14.9 ± 0.503	2932 ± 597	2882 ± 652	2909 ± 440	0.98
KL3D(f)	2.98 ± 0.099	17.9 ± 0.667	3523 ± 714	3470 ± 787	3499 ± 529	0.98
KL3U(a)	3.01 ± 0.125	18.4 ± 0.892	3557 ± 727	3560 ± 815	3558 ± 542	1.00
KL3U(b)	2.46 ± 0.128	15.9 ± 0.854	2908 ± 601	3088 ± 710	2983 ± 459	1.06
KL3U(3)	6.09 ± 0.248	32.3 ± 1.24	7193 ± 1468	6273 ± 1423	6719 ± 1022	0.87
KL3U(4)	2.03 ± 0.136	12.6 ± 0.643	2396 ± 505	2437 ± 559	2414 ± 375	1.02
Surface T3						
KL4D(d)	4.31 ± 0.106	24.3 ± 1.44	5095 ± 1027	4723 ± 989	4902 ± 712	0.93
KL4D(e)	4.5 ± 0.133	24.7 ± 0.85	5312 ± 1074	5015 ± 1032	5158 ± 744	0.94
KL4D(f)	4.81 ± 0.166	28.2 ± 1.09	5681 ± 1153	5483 ± 1127	5580 ± 806	0.97
KL4U(1)	18.9 ± 0.403	119.0 ±3.47	22392 ± 4504	23324 ± 4746	22833 ± 3267	1.04
KL4U(2)	4.27 ± 0.106	23.4 ± 1.05	5037 ± 1015	4683 ± 972	4852 ± 702	0.93
KL4U(4)	4.33 ± 0.172	25.3 ± 1.69	5110 ± 1042	4970 ± 1058	5041 ± 742	0.97

*Sample numbers increase with terrace height. Capital suffix D, and U, refer to downslope (north of fault-trace), and up-slope (south of fault-trace), sampling paths, respectively.

†N.D. is no data.

§Propagated analytical uncertainties include error on the blank, carrier and counting statistics.

#Propagated uncertainties on the model ages include a 20% uncertainty on the production rate.

$Average is a weighted mean of both ^{26}Al and ^{10}Be model ages, $[x]=\left[\sigma^2\right]\sum_{i=1}^{2}\frac{x_i}{\sigma_i^2}$, where $\frac{1}{\left[\sigma^2\right]}=\sum_{i=1}^{2}\frac{1}{\sigma_i^2}$.

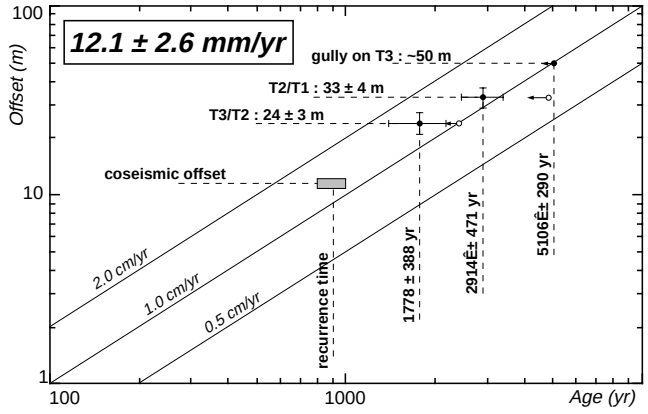

Figure 4. Constraints on late Holocene left-slip rate and recurrence interval of great earthquakes on Xidatan segment of Kunlun fault. Open symbols are minima discussed in text.

view that the imprint of climate change on geomorphology cannot be used to infer ages of chief elements of the landscape in the field or on SPOT images, and hence the order of magnitude of slip rates on active faults (e.g. Ritz et al., 1995).

ACKNOWLEDGMENTS

This study is part of a long-term cooperative program between the Institut National des Sciences de l'Univers (CNRS, Paris, France) and the Ministry of Geology and Mineral Resources (Chinese Academy of Geological Sciences, Beijing, China), initiated by G. Aubert and Xu Zhiqin. We thank those institutions and the French Ministry of Foreign Affairs for financial and logistic support. The Lawrence Livermore National Laboratory (LLNL) group acknowledges support from the Institute of Geophysics and Planetary Physics at LLNL, operating under the auspices of U.S. Department of Energy (DOE) contract ENG-7405. We acknowledge R. J. Weldon and an anonymous reviewer for their constructive comments. This is Institut de Physique du Globe de Paris (IPGP) contribution no. 1538.

REFERENCES CITED

Chang Chenfa, Chen Nansheng, Coward, M. P., Deng Wanming, Dewey, J. F., Gansser, A., Harris, N. B. W., Jin Chengwei, Kidd, W. S. F., Leeder, M. R., Li Huan, Lin Jinlu, Liu Chengjie, Mei Houjun, Molnar, P., Pan Yun, Pan Yusheng, Pearce, J. A., Shackleton, R. M., Smith, A. B., Sun Yiyin, Ward, M., Watts, D. R., Xu Juntao, Xu Ronghua, Yin Jixiang, and Zhang Yuquan, 1986, Preliminary conclusions of the Royal Society and Academia Sinica 1985 geotraverse of Tibet: Nature, v. 323, p. 501–507.

Derbyshire, E., 1987, A history of glacial stratigraphy in China: Quaternary Science Review, v. 6, p. 301–314.

Gasse, F., Arnold, M., Fontes, J. C., Fort, M., Gilbert, E., Huc A., Bingyan, L., Yuanfang, L., Qing, L., Melieres, F., Van Campo, E., Fubao, W., and Qingsong, Z., 1991, A 13 000 year climate record from western Tibet: Nature, v. 353, p. 742–745.

Gaudemer, Y., Tapponnier, P., Meyer, B., Peltzer, G., Guo, S. M., Chen, Z. T., Dai, H. G., and Cifuentes, I., 1995, Partitioning of crustal slip between linked, active faults in the eastern Qilian Shan, and evidence for a major seismic gap, the "Tianzhu gap," on the western Haiyuan fault, Gansu (China): Geophysical Journal International, v. 120, p. 599–645.

Gongxu, G., Tinghuang, L., and Zhenniliangt, S., 1989, Catalogue of Chinese earthquakes (1831 BC–1969 AD): Beijing, China, Science Press.

Kidd, W. S. F., and Molnar, P., 1988, Quaternary and active faulting observed on the 1985 Academia Sinica—Royal Society Geotraverse of Tibet: Philosophical Transactions of the Royal Society, ser. A, v. 327, p. 337–363.

Kohl, C. P., and Nishiizumi, K., 1992, Chemical isolation of quartz for measurement of in-situ produced cosmogenic nuclides: Geochimica et Cosmochimica Acta, v. 56, p. 3583–3587.

Lal, D., 1991, Cosmic ray labeling of erosion surfaces: In situ nuclide production rates and erosion models: Earth and Planetary Science Letters, v. 104, p. 424–439.

Liu Kam-biu, Yao, Z., and Thompson, L. G., 1998, A pollen record of Holocene climatic changes from the Dunde ice cap, Qinghai-Tibetan Plateau, Geology, v. 26, p. 135–138.

Nishiizumi, K., 1989, Cosmic-ray production rate of ^{10}Be and ^{26}Al in quartz from glacially polished rocks: Journal of Geophysical Research, v. 94, p. 17907–17915.

Pachur, H.-J., Wunnemann, B., and Hucai Zhang, 1995, Lake evolution in the Tengger Desert, northwestern China, during the last 40 000 years: Quaternary Research, v. 44, p. 171–180.

Peltzer, G., and Saucier, F., 1996, Present-day kinematics of Asia derived from geologic fault rates: Journal of Geophysical Research, v. 101, p. 27943–27956.

Ritz, J. F., Brown, E. T., Bourlès, D. L., Philip, H., Schlupp, A., Raisbeck, V. M., Yiou, F., and Enkhtuvshin, B., 1995, Slip rates along active faults estimated with cosmic-ray-exposure dates: Application to the Bogd fault, Gobi-Altaï, Mongolia: Geology, v. 23, p. 1019–1022.

Tapponnier, P., and Molnar, P., 1977, Active faulting and tectonics of China: Journal of Geophysical Research, v. 82, p. 2905–2930.

Zhao Guoguang, 1996, Quaternary faulting in North Qinghai-Tibet Plateau: Continental Dynamics, Institute of Geology, Beijing, v. 1, p. 30–37.

Manuscript received December 29, 1997
Revised manuscript received May 7, 1998
Manuscript accepted May 21, 1998